Supporting Information for "The Relationship Between Cloud Radiative Forcing and Surface Temperature at ENSO Frequencies in CMIP5 Models"

N. J. Lutsko,[1]

Contents of this file

1. Text S1

2. Table S1

3. Figures S1 to S5

Introduction The supplementary material contains one text section, one table and six figures. The text provides more details concerning how the spectra were calculated. The

Corresponding author: N. J. Lutsko, Department of Earth, Atmospheric, and Planetary Sciences, Massachusetts Institute of Technology, Cambridge, Massachusetts, USA. (lutsko@mit.edu)

[1]Department of Earth, Atmospheric, and

Planetary Sciences, Massachusetts Institute

of Technology, Cambridge, Massachusetts,

USA.

table lists each model used in the study and the corresponding estimates of β_F and ECS from *Forster et al.* [2013] and *Geoffroy et al.* [2013], the estimates of $\beta_{F,cloud}$ from *Forster et al.* [2013] and the amplitudes from the frequency-dependent regressions, averaged over the $1/2.5$ to $1/3$ years^{-1} frequency band and $\omega = $ -10 to 25hPa/day. The first Figure repeats Figure 2 of the main text, but shows values averaged over the $1/2.5$ to $1/5$ years^{-1} frequency band. The second Figure shows regressions of the Estimate Inversion Strength (EIS) onto the Nino3.4 index for six of the models used in the study. The third Figure shows the phase between $\bar{T}'$ and $L(\omega)'$, averaged over frequencies of $1/2.5$ years^{-1} to $1/3$ years^{-1}. The fourth Figure shows scatter plots of the amplitudes for $C(\omega)'$, averaged between $1/3$ and $1/2.5$ years^{-1} and $\omega = $ -10 to 25hPa/day, and the sensitivity estimates for the models. The fifth Figure repeats the top panel of Figure 4 of the main text, but the regressions are performed using the amplitudes, averaged over frequencies of 2.5 years^{-1} to 3 years^{-1}, for the regressions between $\bar{T}'$ and $P(\omega)'$.

Text S1. As in *Lutsko and Takahashi* [2018], spectra of the model variables were estimated using Thomson's multitaper method [*Percival and Walden*, 1993], which is similar to the more commonly used periodogram method for estimating spectral density. In the periodogram method, rectangular windows are applied to the data, the power of each filtered signal is calculated and the resulting estimates are then averaged together to produce the final estimate of the spectral density. The multitaper method uses a set of optimal windows (tapers), derived from the discrete prolate spheroid sequences, instead of rectangular windows, producing an improved estimate of the spectral density. The number of windows is a free parameter: using more windows reduces the variance of the estimate, however it also produces more spectral leakage. It was found that using eight windows produced good estimates for the data.

References

Forster, P. M., T. Andrews, P. Good, J. M. Gregory, L. S. Jackson, and M. Zelinka (2013), Evaluating adjusted forcing and model spread for historical and future scenarios in the cmip5 generation of climate models, *Journal of Geophysical Research: Atmospheres*, *118*, 1139–1150.

Geoffroy, O., D. Saint-Martin, G. Bellon, A. Voldoire, D. J. L. Olivie, and S. Tyteca (2013), Transient climate response in a two-layer energy-balance model. part ii: Representation of the efficacy of deep-ocean heat uptake and validation for cmip5 aogcms, *Journal of Climate*, *26*(6), 1859–1876.

Lutsko, N. J., and K. Takahashi (2018), What can the internal variability of cmip5 models tell us about their climate sensitivity?, *Journal of Climate*, *31*(13), 5051–5069.

Percival, D. B., and A. T. Walden (1993), *Spectral Analysis for Physical Applications:*

   Multitaper and Conventional Univariate Techniques., 1 ed., Cambridge University Press.

Silvers, L. G., D. Paynter, and M. Zhao (2018), The diversity of cloud responses to

   twentieth century sea surface temperatures. *Geophysical Research Letters*, *45*, 391–400.

Wood, R. (2006), Review: Stratocumulus Clouds,*Monthly Weather Review, 140*12, 233–

   2423.

Table S1.   The models used in this study and their corresponding β_F and ECS estimates from *Forster et al.* [2013] (F13) and *Geoffroy et al.* [2013] (G13). The fourth column shows the $\beta_{F,cloud}$ estimates from *Forster et al.* [2013] and the fifth column shows the amplitudes, averaged over the 1/2.5 to 1/3 years^{-1} frequency band and ω = -10 to 25hPa/day (a).

Model	β_F (F13)/(G13) [Wm^{-2}K^{-1}]	ECS (F13)/(G13) [K]	β_{CF} [Wm^{-2}K^{-1}]	a [Wm^{-2}K^{-1}5hPa^{-1}]
BCC-CSM1-1	-1.14/-1.28	2.82/2.9	-0.07	0.067
BNU-ESM	n.a./-0.92	n.a./3.9	n.a	0.038
CanESM2	-1.04/-1.06	3.69/3.9	0.13	0.046
CNRM-CM5	-1.14/-1.12	3.25/3.2	-0.20	0.008
CSIRO-Mk3-6-0	0.63/-0.68	4.08/5.1	0.23	0.081
FGOALS-s2	-0.92/-0.87	4.17/4.5	-0.48	0.051
GFDL-CM3	-0.7/n.a.	3.97/n.a.	0.48	0.059
GFDL-ESM2G	-1.29/n.a.	2.39/n.a.	-0.26	0.041
GFDL-ESM2M	-1.38/-1.38	2.44/2.5	-0.33	0.038
GISS-ESM-LR	-1.79/-2.03	2.11/2.25	-0.48	0.009
HADGEM2-ES	-0.64/-0.61	4.59/5.5	0.37	0.050
INMCM4	-1.43/-1.56	2.08/1.9	-0.12	0.039
IPSL-CM5A-LR	-0.75/-0.79	4.13/4.25	0.7	0.058
MIROC5	-1.52/-1.58	2.72/2.8	-0.51	0.012
MPI-ESM-LR	-1.13/-1.21	3.63/3.9	-0.04	0.022
MRI-CGCM3	-1.25/-1.31	2.60/2.7	-0.09	0.043
NCAR-CCSM4	-1.23/-1.4	2.89/3.0	-0.16	0.032
NorESM1-M	-1.11/-1.15	2.80/3.25	-0.11	0.050
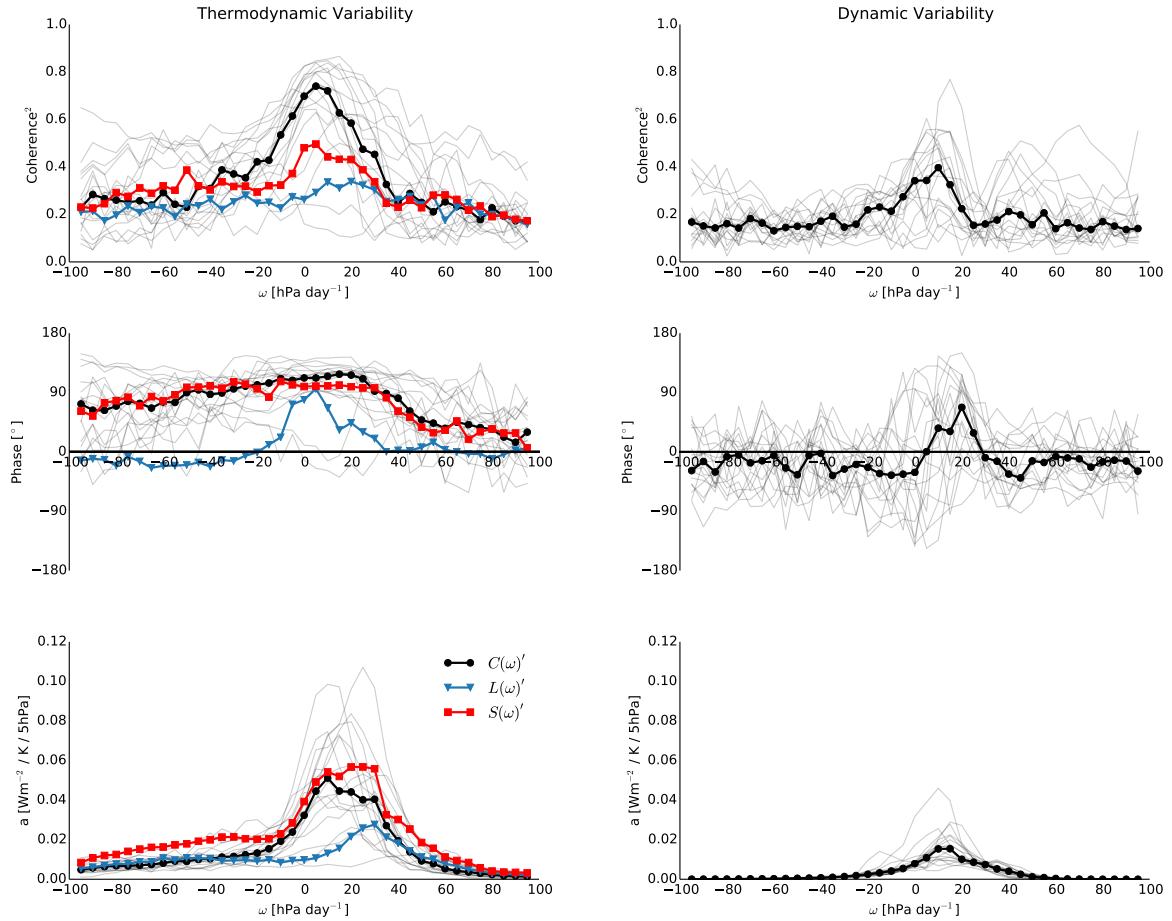
Figure S1.   As in Figure 2 of main text but the values are averaged over frequencies of $1/2.5$ to $1/5$ years^{-1} rather than $1/2.5$ to $1/3$ years^{-1}.
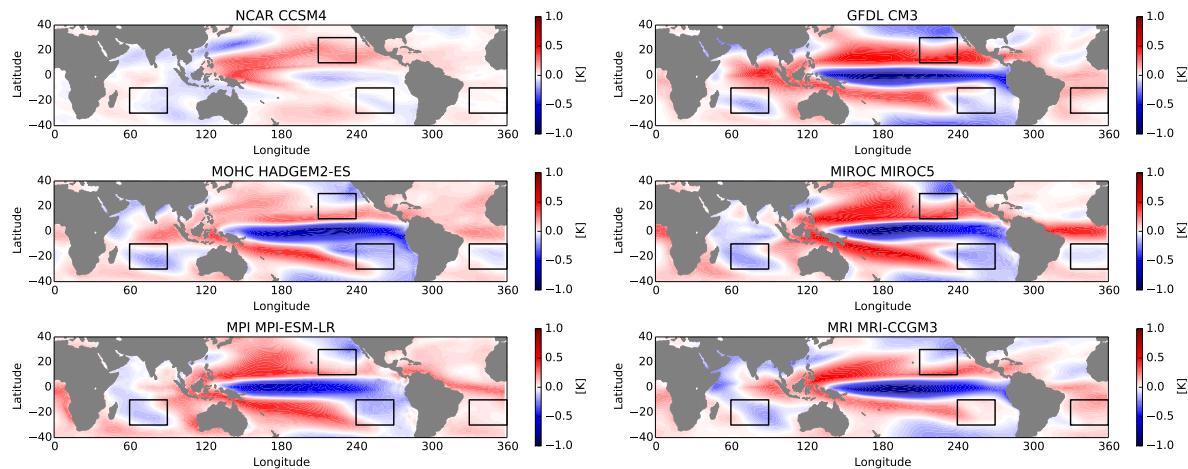
Figure S2.   Regression of the Estimated Inversion Strength (EIS) onto the Nino3.4 index in six of the CMIP5 models, using monthly data. The EIS is computes as: $EIS = LTS - \Gamma_m^{850}(z_{700} - LCL)$ where LCL is the lifting condensation level, Γ is the moist adiabatic lapse-rate, z is the geopotential height and LTS is the lower tropospheric stability. All variables are calculated as in *Silvers et al.* [2018], and positive values inducate that low cloud cover is enhanced during positive El Niño events. The boxes highlight regions which have been identified in observations as being important for stratocumulus clouds [*Wood*, 2006].
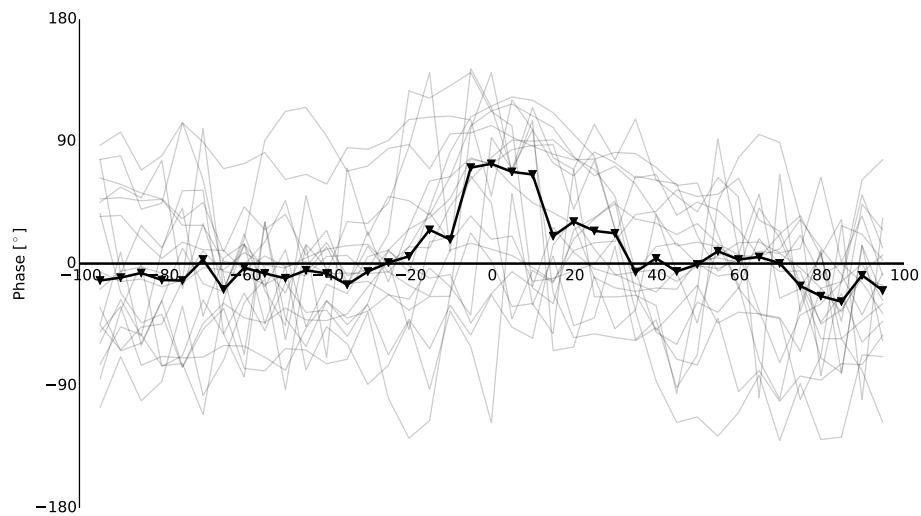
Figure S3.   As in the middle panels of Figure 2 of the main text, but only showing the phase between $\bar{T}'$ and $L(\omega)'$. The individual models are in gray and the ensemble median is shown by the thick black line.
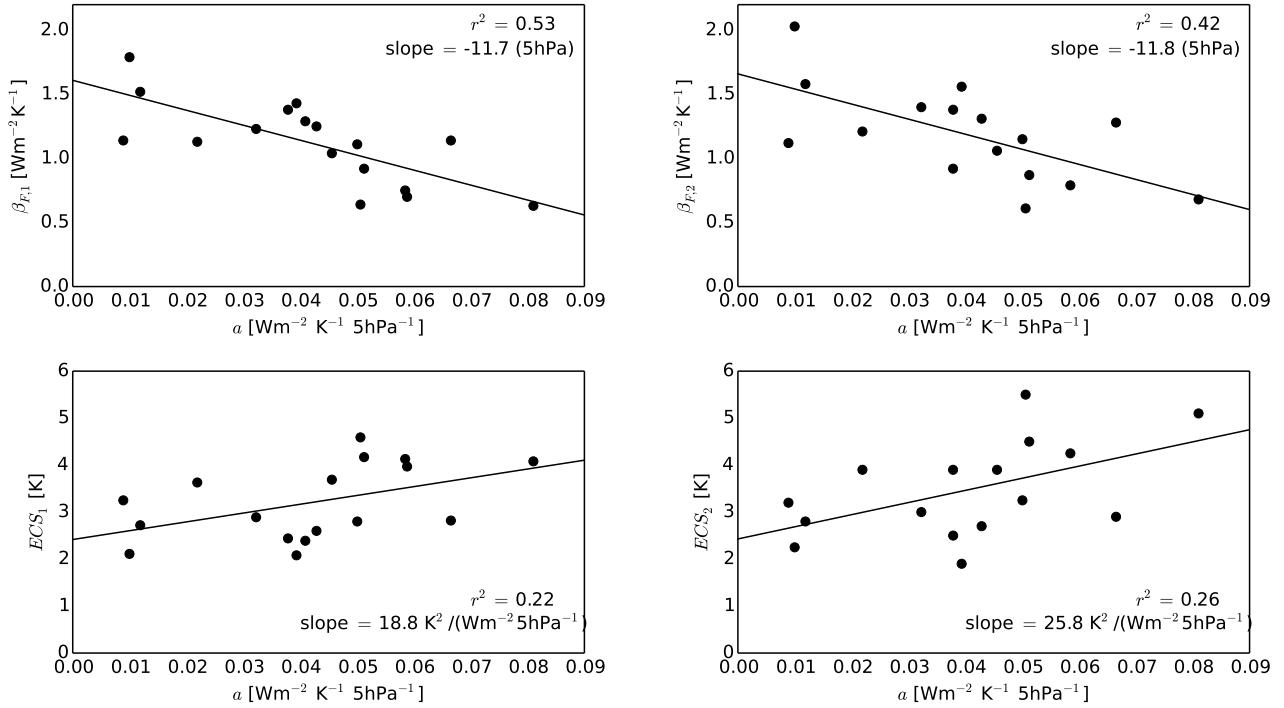
Figure S4. Top left panel: scatter plot of the amplitudes for $C(\omega)'$ averaged between 1/3 and 1/2.5 years^{-1} frequency and ω = -10 to 25hPa/day versus the $\beta_{F,1}$ estimates. Top right panel: same for the $\beta_{F,2}$ estimates. Bottom left panel: same for the ECS_1 estimates. Bottom right panel: same for the ECS_2 estimates.
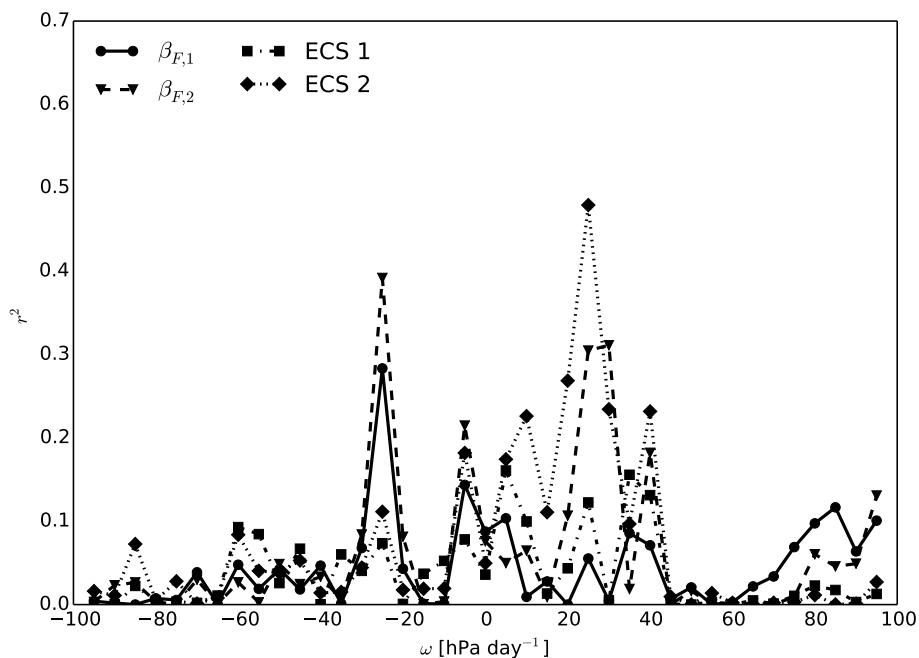
Figure S5.   As in Figure 4 of the main text but the r^2 values are now for the amplitudes from regressions between $\bar{T}'$ and $P(\omega)'$.